Journal of Hazardous Materials 209–210 (2012) 256–263

Contents lists available at SciVerse ScienceDirect

Journal of Hazardous Materials

journal homepage: www.elsevier.com/locate/jhazmat

Characterization of chitosan/montmorillonite membranes as adsorbents for Bezactiv Orange V-3R dye

Aleksandra R. Nesic[a,*], Sava J. Velickovic[b], Dusan G. Antonovic[b]

[a] Vinca Institute of Nuclear Sciences, University of Belgrade, PO Box 522, RS – 11001 Belgrade, Serbia
[b] Faculty of Technology and Metallurgy, University of Belgrade, Karnegijeva 4, Belgrade 11000, Serbia

ARTICLE INFO

Article history:
Received 9 October 2011
Received in revised form
20 December 2011
Accepted 4 January 2012
Available online 20 January 2012

Keywords:
Chitosan
Montmorillonite
Adsorption
Membranes
Azo dye

ABSTRACT

The synthesis, characterization and environmental application of chitosan/montmorillonite membrane for adsorption Bezactiv Orange V-3R were investigated. Chitosan/montmorillonite membranes were synthesized in different ratios, containing 10–50% of montmorillonite (MMT) in membrane. These membranes were characterized by using Fourier transform infrared spectroscopy (FTIR), thermogravimetry (TG) and scanning electron microscopy (SEM). The adsorption kinetics were investigated using three different concentrations of Bezactiv Orange dye (30, 50 and 80 mg/L). The adsorption capacity increases with increasing amount of MMT in membranes. These membranes show the highest adsorption capacity when the initial dye concentration was 80 mg/L. The results show that the optimum condition for adsorption of Bezactiv Orange is pH 6. A comparison of kinetic models was evaluated for the pseudo-first and pseudo-second order and intra-particle diffusion. The experimental data were fitted to the pseudo-second order kinetic model, and also followed by intra-particle diffusion. Intra-particle diffusion is not the only rate-controlling step. The Langmuir and Freundlich adsorption isotherms were applied to experimental equilibrium data at different concentration of dye solution. The results indicated the competency of chitosan/MMT membranes adsorbent for Bezactiv Orange adsorption.

1. Introduction

Synthetic dyes are among the most commonly used pollutants which appear in various industries, such as dyestuff, textiles, leather, and paper [1]. The dyes exhibit a wide range of different chemical structures, primarily based on substituted aromatic and heterocyclic groups. A large number of dyes are azo compounds that are linked by an azo bridge [2]. The removal of these dyes from water is very important from an environmental point of view. Even very low concentration of the dyes present in water can be highly toxic to aquatic systems [3]. The most efficient method for the removal of azo dyes from aqueous effluents is adsorption [4], where one of the most widely used adsorbents, due to its high adsorption capacity is, activated carbon [5–7]. However, it is expensive and difficult to regenerate. From this point on, much attention has recently been focused on biosorbent materials [8–11] – those that are not expensive, can be obtained from renewable resources, and are harmless to nature. Special attention has been given to polysaccharides such as chitosan – the deacetylated form of chitin, which is a linear polymer of acetylamino-D-glucose. Chitosan has excellent properties for adsorption of anionic dyes, principally due to the presence of protonated amino groups ($-NH_3^+$) in the polymer matrix, which interact with dyes in solution by ion exchange at an appropriate pH [1,12,13]. Removal of dyes using chitosan has its drawbacks as its effectiveness as adsorbent is strongly pH dependent. Chitosan effectively removes dyes at acidic pH, so the pH of the wastewater has to be adjusted on the acidic side, before treatment. The other attractive adsorbents are clays, due to their low cost and their abundance in various parts of the world [14–20]. Clays themselves have some sorption capabilities, so combining clays with chitosan can produce a very good sorbent, at the same time decreasing the chitosan drawbacks. Since each chitosan unit possesses one amino and two hydroxylic groups, these functional groups can form hydrogen bonds with the silicate hydroxylated end groups of clay, leading to strong interaction between chitosan and clay. The formation of hydrogen bonds between chitosan and clay is represented in Fig. 1. Dissolution of chitosan in acetic acid resulted in reaction between amine group from chitosan and acetic acid residue ($NH_3^+Ac^-$). Chitosan hydroxyl group form hydrogen bonds with Si—O—Si groups of silicate multilayer of montmorillonite (MMT). Nanocomposites of chitosan and MMT have been already tested as electrochemical sensors [21], as adsorbents for

* Corresponding author. Tel.: +381 11 2455654; fax: +381 11 3370387.
E-mail address: anesic@vin.bg.ac.rs (A.R. Nesic).

0304-3894/$ – see front matter © 2012 Elsevier B.V. All rights reserved.
doi:10.1016/j.jhazmat.2012.01.020

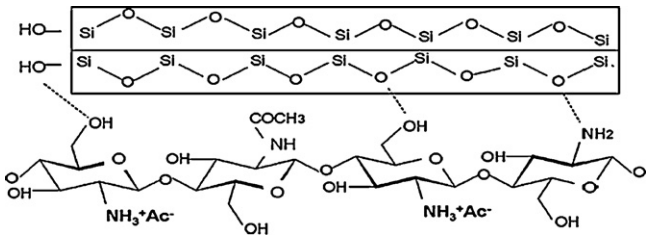

Fig. 1. Complexation between chitosan and MMT.

tannic acid [22], and for controlled release of ofloxacin [23]. The beads of chitosan/MMT were studied for removal of Reactive Red 120 [24], Basic Blue 9, Basic Blue 66 and Basic Yellow 1 [25].

In the present study, the membranes of chitosan and MMT were obtained to improve the chitosan adsorption capability. Adsorption was tested with Bezactiv Orange V-3R (BO). The effects of different amount of MMT in membrane, pH and temperature on the adsorption of BO were evaluated.

2. Experimental

2.1. Materials

Chitosan (low viscous) was obtained from Acros Organic and used without any further purification. According to the producer data, its molecular weight is about 100 000–300 000 g/mol. The degree of deacetylation, determined by potentiometric titration [26], is 80%. Cloisite Na+ was a natural sodium-rich MMT obtained from Southern Clay Products Inc. (USA). Bezactiv Orange V-3R (or known as Remazol Brilliant Orange 3R) (Fig. 2) was a gift from Bezema AG.

2.2. Synthesis of chitosan/montmorillonite membranes

Chitosan/montmorillonite membranes were prepared by mixing solutions of chitosan and montmorillonite in different ratios. The montmorillonite amount was from 10% to 50% by mass. The general procedure of synthesis is as follows: chitosan (1 wt%) was dissolved in 0.2 M acetic acid with constant stirring at the temperature of 50 °C. Montmorillonite was dispersed in 0.2 M acetic acid with constant stirring 30 min at the temperature of 50 °C. These solutions were mixed with constant stirring 30 min. The mixed solutions in different ratios of MMT were cast on Petri dishes and left to evaporate at room temperature for 24 h.

2.3. Characterization of membranes

2.3.1. Instrumental analysis

FTIR spectra of chitosan/montmorillonite membranes before and after adsorption azo dyes were recorded on a Bomem MB 100 FTIR spectrophotometer from KBr pellets.

Thermogravimetry (TG) was performed by a SDT Q-600 TG instrument (TA Instruments). All analysis were performed with 5 mg samples in ceramic pans under nitrogen atmosphere between 0 and 600 °C at heating rate 10 °C/min.

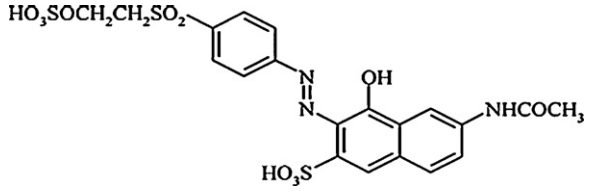

Fig. 2. Bezactiv Orange V-3R.

SEM-EDX was used to determine morphology of membranes before and after adsorption azo dyes. Measurements were taken on a JEOL JSM-5800 scanning electron microscope.

The dye concentrations were measured at a wavelength $\lambda = 493$ nm by UV/VIS Shimadzu 1700 spectrophotometer.

2.4. Dye adsorption batch experiments

Experiments were carried out by adding between 12 and 18 mg of membrane into 50 ml of dye solution with desired concentration, temperature of solution and appropriate pH. As the kinetics of adsorption were not dependent on membrane mass, it was possible to use this relatively wide range of membrane masses. The effect of dye concentration was investigated at pH 6, at 20 °C and from 30 to 80 mg/L. For pH studies, 50 ml of 80 mg/L of dye solution was adjusted to various pH ranging from 4 to 7.4. The effect of temperature on adsorption of dyes was studied at 8, 20, 37 and 55 °C at 80 mg/L dye concentration. Preliminary studies showed that the dye adsorption was completed within 4 days. The capacity of adsorbed dye was calculated according to the following equation:

$$q_e = (C_0 - C_e)\frac{V}{m} \quad (1)$$

where q_e (mg/g) is the amount of dye adsorbed on the membrane, C_0 (mg/L) the initial concentration of dye, C_e the equilibrium concentration of dye in solution, V (L) the volume of the used dye solution and m (g) the weight of the used membrane.

Each experiment was repeated three times under the same controlled conditions.

2.5. Kinetic experiments

Kinetic experiments were conducted in order to determine the time needed to reach equilibrium and adsorption rates of dye. The effect of concentration on sorption kinetics was investigated, following the above described methodology: 50 ml of three different concentration of dye solution (30,50,80 mg/L) were prepared. Three milliliter samples were taken periodically during 4 days and analyzed by UV/vis. The data were modeled using both first- and second-order kinetic models. The pseudo-first-order model assumes that the rate of change of surface site concentration is proportional to the amount of remaining unoccupied surface sites:

$$\frac{dq}{dt} = k_1(q_e - q) \quad (2)$$

where q and q_e are the adsorbed amounts (mg/g) at time t and equilibrium, respectively, and k_1 (h^{-1}) the first-order Lagergren adsorption rate constant [27]. This model can be linearized as:

$$\log(q_e - q) = \log q_e - \frac{k_1}{2.303} \times t \quad (3)$$

The pseudo-second-order model assumes that the rate is proportional to the square of the number of remaining free surface sites [28]:

$$\frac{dq}{dt} = k_2(q_e - q)^2 \quad (4)$$

with the second-order adsorption rate constant k_2. This model can be linearized as:

$$\frac{t}{q} = \frac{1}{k_2 q_e^2} + \frac{t}{q_e} \quad (5)$$

The pseudo-first and pseudo-second order kinetic models cannot identify the diffusion mechanism, so kinetic results need to be analyzed by using the intra-particle diffusion model. In the

model developed by Weber and Morris [29], the initial rate of intra-particle diffusion is calculated by linearization of equation:

$$q_t = k_p t^{0.5} + C \quad (6)$$

where C is the intercept and k_p the ultra-particle diffusion rate constant ($mg/g\,h^{1/2}$).

3. Results and discussion

3.1. FTIR spectroscopy

Fig. 3 shows the FTIR spectra of chitosan, Na^+ montmorillonite, and chitosan/montmorillonite with amounts of montmorillonite in membrane of 10, 30 and 50%, and the membranes with 50% MMT after dye adsorption from solutions containing 30, 50 and 80 mg/L.

FTIR spectrum of MMT shows bands at 3631 cm^{-1} and 3435 cm^{-1} which are assigned to the water belonging to the original clay structure and stretching vibrations of hydroxyl group, respectively. Three bending vibrations of hydroxyl groups at 911 cm^{-1} (AlAlOH), 880 cm^{-1} (AlFeOH) and 846 cm^{-1} (AlMgOH) confirm the substitution in octahedral layer. The band at 1635 cm^{-1} is the bending vibration of hydroxyl group from water molecules present in the clay. The strong bands located in the range of 1160–1045 cm^{-1} refer to Si—O—Si moiety and stem from stretching. The band at 530 cm^{-1} indicates bending vibration of Si—O. These peaks for MMT are confirmed in literature [25,30].

In order to characterize the initial material, a spectrum of pure chitosan was also recorded. FTIR spectrum of chitosan powder shows characteristic hydroxyl group at 3440 cm^{-1}, and stretching vibrations of C=O group at 1740 cm^{-1}. The bending vibrations of C—H bond in $-CH_2$ are located at 2930 cm^{-1} and in $-CH_3$ group are located at 2845 cm^{-1} [31,32]. The band at 1635 cm^{-1} is related to the stretching vibrations of amide group carbonyl bonds C=O and the band at 1540 cm^{-1} is related to the stretching vibrations of amine group [33]. Bending vibrations of methylene and methyl groups are located at 1380 cm^{-1} and 1460 cm^{-1}, respectively. The spectrum in the range from 1150 to 1000 cm^{-1} is attributed to stretching vibrations of C—O groups [34].

The characteristic bands needed to confirm complexation between chitosan and MMT are shifted to the higher frequency. The characteristic MMT bands appear at 3742 cm^{-1} (–OH), near the 3445 cm^{-1} (hydroxyl group from MMT and chitosan), in a range of 1118–1040 cm^{-1} (stretching vibrations of Si—O), and bending vibration of Si—O at 523 cm^{-1}. Characteristic amide group from chitosan located at 1635 cm^{-1} is shifted to higher frequencies, to 1645 cm^{-1}. The peak located at 1540 cm^{-1}, which corresponds to the NH_2– group form chitosan, is shifted to higher frequency, 1560 cm^{-1}, indicating that the acetic acid residue (CH_3COO–) is attached to amine group in the chitosan chain [35]. The shift of amide and amine group can be related to the electrostatic interaction between these groups and the negatively charged sites in the clay structure, which confirm complexation between chitosan and MMT [25,36,37].

The changes in the FTIR spectrum of the membranes after binding with the dye are significant. The –OH stretching, observed as strong band at 3445 cm^{-1} in unloaded membrane, shifts to 3430 cm^{-1} after binding azo dye. The shift of amide and C=O bands are also observed for loaded membrane (1629 cm^{-1}, and 1720 cm^{-1}, respectively). Characteristic MMT bands in membrane are shifted too. The peaks of Si—O in-plane and out-of-plane stretching vibration are shifted from 1040 cm^{-1} to 1034 cm^{-1}, and from 1118 cm^{-1} to 1123 cm^{-1}, respectively. The new strong band that appeared in all FTIR spectra of chitosan/MMT membranes around 1590 cm^{-1} indicates azo group [38]. These results confirm that $-CONH_2$, $-NH_2$ and –OH groups from chitosan, and Si—O group from MMT are involved in binding of azo dye.

Table 1
The relevant TG parameters for chitosan/MMT membranes, W_1: weight loss for the first degradation peak (%), W_2: weight loss for the second degradation peak (%).

Sample	W_1 (%)	W_2 (%)	Tg (°C)
Chitosan	5.4	93.0	240
Chitosan/MMT 10%	14.4	45.0	286
Chitosan/MMT 50%	12.0	40.0	275

3.2. Thermogravimetry

The previous investigations have shown that the decomposition of chitosan has 2 endothermic processes, the first one around 60 °C for water evaporation, and the second one starts around 220 °C and reaches a maximum 240 °C [39].

It is known from the literature [39] that although MMT increases thermal stability of chitosan/MMT, this effect is most pronounced at low amounts of MMT in the system, while at higher loads of MMT the decomposition temperature decreases. This is the result of formation of parallel monolayers of MMT that can form strong electrostatic interactions with chitosan. The higher loads of clay decrease the regularity of the structure, and thus decrease the strength of electrostatic interactions. We have observed the same trend in this investigation, so the main degradation peak in DTG diagrams, that is attributed to thermal degradation and deacetylation of chitosan [40,41] for membrane containing 50% of MMT is located at a temperature nine degrees lower than for the 10% MMT membrane (Table 1, Fig. 4). It is also visible that in case of 10% MMT sample, the adsorbed water molecules, that are reported to start to desorb at around 150 °C [39,42], desorb at much higher temperature than in the 50% MMT sample which is probably also the result of more uniform structure when lower loads of MMT are present. Concerning the residue at 600 °C, in case when 50% MMT was initially present the residue is in accordance with it – i.e. it is about 50% indicating that the complete organic phase has decomposed. When only 10% of MMT was initially present, the residue is over 30% indicating the existence of charred residue of organic phase. It can be attributed to abovementioned parallel monolayers that form at higher loads of clay that prevent formation of charred residue. When the loads of clay are lower, parts of chitosan tend to char during degradation. Thermal degradation of pure chitosan, as earlier investigations show, can have charred residue of up to 40% at 600 °C [40].

3.3. Scanning electron microscopy

SEM analysis of unloaded and loaded membranes chitosan/montmorillonite with amount of MMT 50% in membrane were recorded at Fig. 5.

SEM is a widely used technique to study morphology and surface characteristics of the adsorbent. In the present study, SEM is used to assess morphological changes in chitosan/MMT membrane surface after adsorption of Bezactiv Orange. It is visible from micrographs that the samples with lesser amount of MMT have smooth surface, while after adsorption a nonuniform white layer appears, together with roughening of the surface. With increase of MMT amount the surface becomes rougher, more homogenous, with numerous bulk-like agglomerates protruding. After the adsorption the aforementioned layer that we assume to be adsorbed dye appears again in these samples as well.

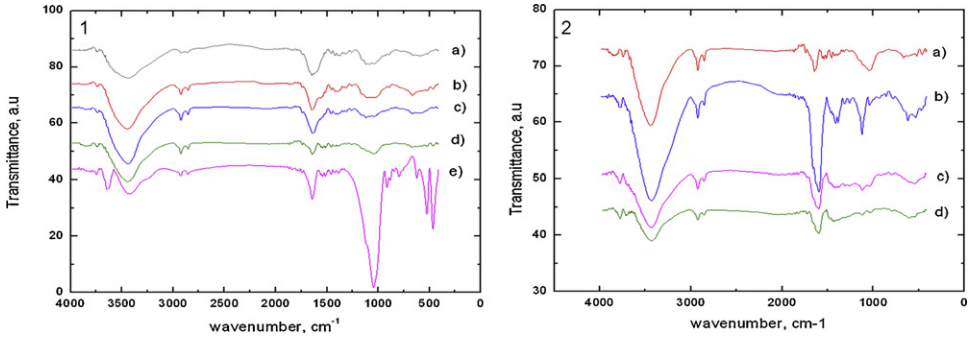

Fig. 3. FTIR spectra of: 3.1. a) pure chitosan, b) chitosan/MMT membrane with amount of MMT of 10% in membrane, c) 30% MMT in membrane, and d) 50% MMT in membrane, e) pure MMT; 3.2. a) chitosan/MMT 50%, b) chitosan/MMT 50% with concentration of dye of 30 mg/L, c) chitosan/MMT 50% with concentration of dye 50 mg/L, and d) chitosan/MMT 50% with concentration of dye of 80 mg/L.

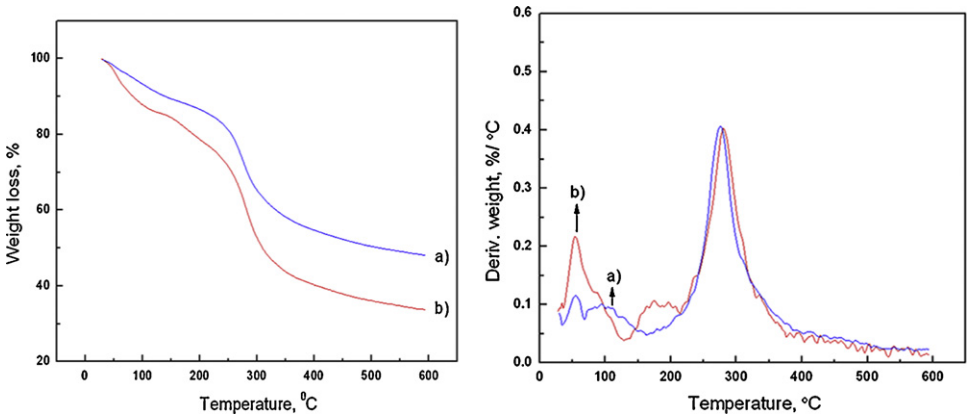

Fig. 4. TG and DTG of chitosan/MMT membranes with content of MMT in membrane: a) 50%; b) 10%.

3.4. Effect of dye concentration

The dye adsorption kinetic was studied at three different concentrations: 30, 50 and 80 mg/L. The time needed for the samples to equilibrate was found to be 4 days. The experimental results demonstrating the effect of initial concentration of dye on the removal by chitosan/MMT membranes are shown in Fig. 6.1, 6.2, 6.3, 6.4. Although it may seem that no plateau exists in some of the diagrams, the final experimental point in represents the value where the plateau was obtained.

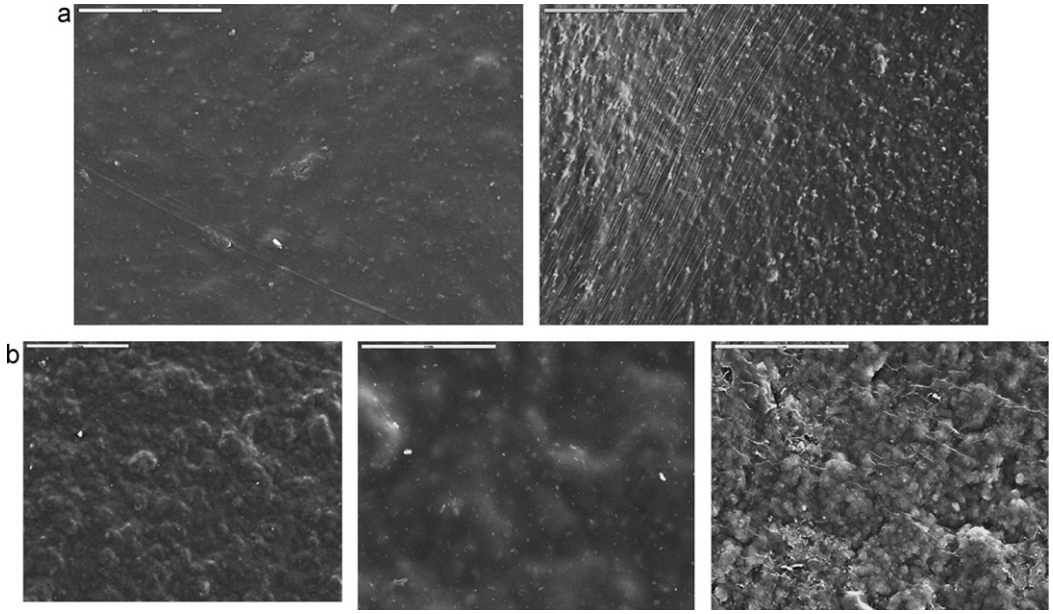

Fig. 5. a) SEM morphologies of chitosan/MMT 10% membrane before and after adsorption of dye, increasing 200 μm; b) SEM morphology of chitosan/MMT 50% membrane: a) before adsorption, increasing 50 μm, b) increasing 200 μm, and c) after adsorption of dye, increasing 200 μm.

Table 2
Kinetic parameters of chitosan/MMT membranes at different concentration of dye, k_2: rate constant for pseudo-second order (g mg^{-1} h^{-1}); Q_{max}: maximum capacity of adsorption (mg/g); and k_{p2}: rate constant for intra-particle diffusion (g mg^{-1} h$^{-1/2}$).

Sample	Concentration (ppm)	Pseudo-first order	Pseudo-second order			Intra-particle diffusion	
		R^2	R^2	k_2	Q_{max}	k_{p1}	k_{p2}
Chitosan/MMT 10%	30	0.99	0.99	0.00255	64.4	18.5	4.9
Chitosan/MMT 20%		0.98	0.99	0.00249	65.9	18.9	5.3
Chitosan/MMT 30%		0.93	0.99	0.00353	67.7	20.9	5.1
Chitosan/MMT 40%		0.96	0.99	0.00217	76.5	22.1	4.4
Chitosan/MMT 50%		0.99	0.99	0.00231	71.2	20.4	4.5
Chitosan/MMT 10%	50	0.85	0.98	0.00183	90.1	32.4	6.6
Chitosan/MMT 20%		0.58	0.97	0.00186	98.9	37.8	6.2
Chitosan/MMT 30%		0.89	0.99	0.00119	126.7	38.6	7.1
Chitosan/MMT 40%		0.62	0.99	0.000537	160.5	31.2	7.3
Chitosan/MMT 50%		0.95	0.99	0.000168	152.5	53.5	23.5
Chitosan/MMT 10%	80	0.84	0.99	0.00267	143.4	53.8	7.7
Chitosan/MMT 20%		0.79	0.99	0.00120	155.7	97.0	7.2
Chitosan/MMT 30%		0.84	0.99	0.000550	230.9	110.7	14.4
Chitosan/MMT 40%		0.92	0.99	0.000457	279.3	115.0	27.4
Chitosan/MMT 50%		0.91	0.99	0.000258	242.1	112.0	39.9

The adsorption capacity increases with increasing amount of MMT in membranes. Depending on the dye concentration the differences in adsorption capacity move from negligible at 30 mg/L of dye, to obvious at 80 mg/L. It is interesting to note that the highest capacity was in fact observed at 40% MMT (not shown in the figure), that was slightly higher than the capacity of membrane with 50% MMT. It was reported in the literature that increasing the mass ratio of MMT > 50% in chitosan/MMT complexes could not form stable composite [24]. The increase of dye concentration in solution increases adsorption capacity, and it reaches maximum from 80 mg/g for lower concentration of 30 mg/L of dye to 152 mg/g for concentration of 50 mg/L of dye, and 280 mg/g for concentration of 80 mg/L of dye.

3.5. Adsorption kinetics

Kinetics of adsorption were modeled by the first order Lagergren equation, the pseudo-second order equation and intra-particle diffusion equation. Parameters of the kinetic models were estimated from experimental data and represented in Table 2.

3.6. Intra-particular diffusion

The dependencies of q_t vs. $t^{1/2}$ are shown in Fig. 6.5 at different concentration of dye. As can be seen from Fig. 6.5, the plots consist of three linear sections with different slopes. A similar multilinearity has been observed in other systems for the dye

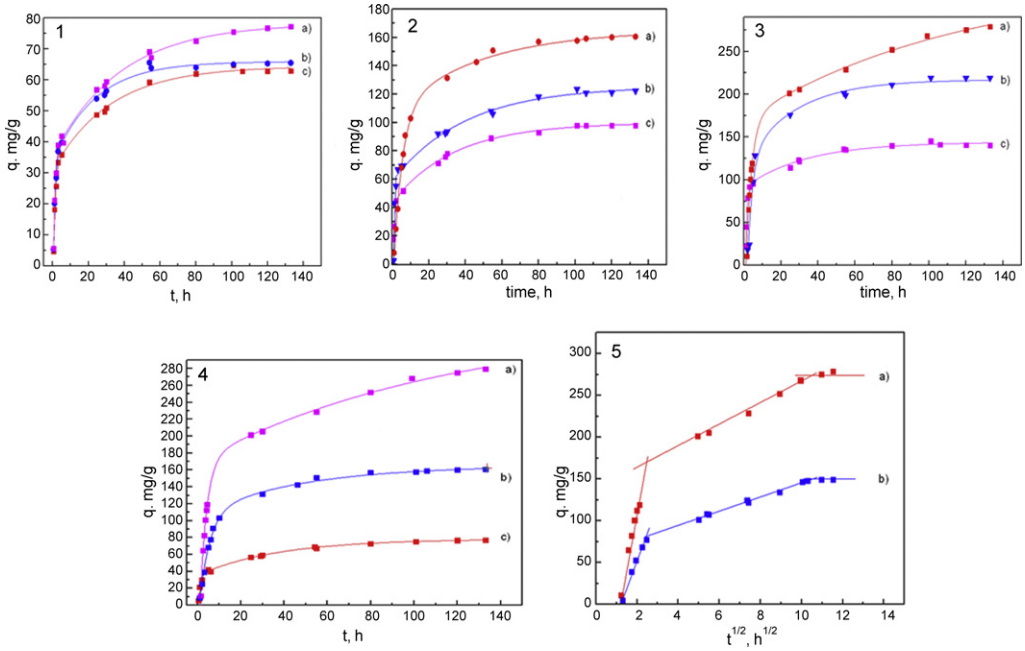

Fig. 6. Adsorption kinetics of Bezactiv Orange onto chitosan/MMT membranes with content of MMT in membrane: a) 40%, b) 30%, and c) 10%. Initial conditions: concentration of dye: 6.1 30 mg/L, 6.2 50 mg/L, 6.3 80 mg/L; 6.4 adsorption kinetics of Bezactiv Orange onto chitosan/MMT membranes with content of MMT in membrane 40%, and concentration of azo dye: a) 80 mg/L, b) 50 mg/L, and c) 30 mg/L; 6.5 intra-particle diffusion model of chitosan/MMT membranes with content of MMT 40% at different concentration of dye: a) 80 mg/L and b) 50 mg/L. pH 6, weight of adsorbent in a range of 12–18 mg.

Table 3
The rate constants of intra-particle diffusion related to the adsorption of Bezactiv Orange by chitosan/MMT membranes at different concentrations of dye.

Sample	Q_{max} (mg/g)			
	8 °C	20 °C	37 °C	55 °C
H/MMT 10%	144.5	143.5	153.8	141.8
H/MMT 20%	198.6	155.7	156.5	157.9
H/MMT 30%	245.3	230.9	221.5	167.2
H/MMT 40%	300.5	279.9	246.3	180.6
H/MMT 50%	280.2	242.1	232.7	171.3

adsorption on porous titania aerogel [43], sepiolite [17], montmorillonite and other organic clay [19], chitosan [13], modified chitosan with polyvinyl alcohol [44]. This reveals that three stages are taking place. The first stage is attributed to the external surface adsorption correlated to the boundary layer diffusion. The second stage is slower than the first one, and is attributed to the intra-particle diffusion. The second stage linear dependency did not pass trough zero, which indicates that intra-particle diffusion is involved in the adsorption process, but is not the only rate controlling step. The third stage refers to the final equilibrium stage.

Comparison of kp values (Table 2) reveals that the first diffusion stage is fastest and that the rate rapidly grows with the dye concentration increase. The second diffusion stage is slower than the first one. As the departure from the intra-particular mechanism indicates some influence of boundary layer diffusion control it is likely that the concentration of dye impairs the ability of molecules to approach the surface, thus influencing the rate of adsorption.

As seen from Table 2, the calculated correlation coefficients are closer to unity for pseudo-second order kinetic model then for the first order kinetic model. Therefore, it was ascertained that the pseudo-second order equation best describes the dye adsorption on chitosan/MMT membranes. A good agreement with this adsorption model is confirmed by the similar values of calculated Q_{max} and experimental ones for all investigated adsorbents.

3.7. Effect of temperature

The best fit to the pseudo-second order kinetics indicates that the adsorption of dye decreases with increase of solution temperature. These results may be attributed to the fact that the increase of solution temperature reduces the time needed for the samples to equilibrate, but decreases the adsorption capacity due to the ability of ions at high temperature as well [45]. In our case, the adsorption capacity decreased with solution temperature increase for the samples with 30, 40 and 50% amount of MMT in membrane (Table 3). On the other hand, the solution temperature had a slight effect on adsorption capacity for samples with 10 and 20% amount of MMT in membrane.

3.8. Effect of pH

The pH value of due adsorption plays an important role in adsorption process and has great influence on the adsorption capacity. The effect of pH on Bezactiv Orange dye removal by chitosan/MMT membranes is shown in Fig. 7. Dye adsorption increases by increasing of pH and reaches maximum at pH 6 and then decreases in alkaline solution. These results can be explained by following observations: At acidic pH the anionic dye bearing sulfonic groups, is electrostatically attracted by protonated amine groups, thus neutralizing the anionic charges of dyes that can bind together. The removal of the dye reached maximum with the complete neutralization of the anionic charges. In alkaline solutions, deprotonation of amine group takes place and results in poor interaction between dye and adsorbent. Similar results were reported by Singh et al. [46] for adsorption of Remazol Violet on poly(acrylamide) functionalized chitosan, and on poly(methyl methacrylate) grafted chitosan [47].

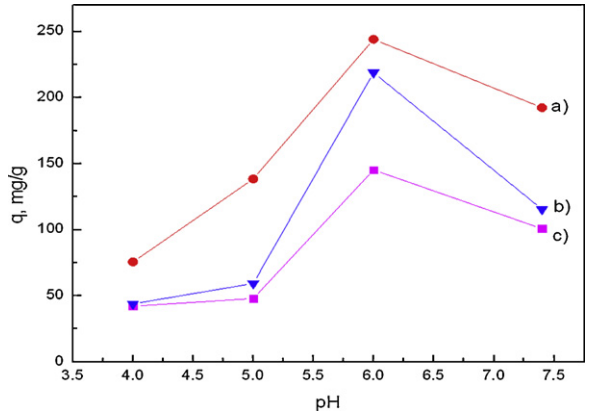

Fig. 7. pH effect on the adsorption capacity of Bezactiv Orange (80 mg/L) on chitosan/MMT membranes with content of MMT in membrane: a) 50%, b) 30%, and c) 10%.

3.9. Adsorption isotherms

Isotherms were obtained by varying the initial concentration of azo dye from 20 to 70 mg/L. An equilibrium time of 4 days was allowed. Adsorption data were fitted to the Langmuir and Freundlich isotherms.

The Langmuir isotherm is adequate for monolayer sorption, and considers that the sorbent surface contains only one type of binding site and sorption of one ion per binding site is taking place. The Langmuir isotherm is expressed by following equation:

$$q_e = K \times q_{max} \frac{C_e}{1 + K \times C_e} \quad (9)$$

where q_e is the amount adsorbed at equilibrium (mg/g), q_{max} (mg/g) the monolayer adsorption capacity, K (L/mg) the Langmuir constant related to adsorption energy, and C_e the equilibrium concentration (mg/L). The Langmuir parameters can be determined from linear form of equation:

$$\frac{C_e}{q_e} = \frac{1}{Kq_{max}} + \frac{C_e}{q_{max}} \quad (10)$$

The Freundlich isotherm describes the heterogeneous surface energies by multilayer adsorption. The Freundlich isotherm is expressed as:

$$q_e = k_f Ce^{1/n} \quad (11)$$

where k_f indicates adsorption capacity (mg/g), and n empirical parameter related to the intensity of adsorption which varies with the heterogeneity of the adsorbent. The value n is always greater than 1, so exponent $1/n$ represents the intensity of adsorption and heterogeneity in a range between 0 and 1. The high n values for isotherms indicate relative uniformity at the surface, whereas low values suggest high adsorption at low concentrations in solution. Furthermore, low values of n indicate the existence of a higher proportion of active sites with high energy [48].

The Freundlich parameters can be determined from linear form of equation:

$$\log k_e = \log k_f + \frac{1}{n} \log C_e \quad (12)$$

The isotherms data were analyzed and the list of the obtained parameters is provided in Table 4. A comparison the experimental data with adsorption isotherms showed that the Freundlich equation represented the better fit of experimental data ($R^2 = 0.99$) than

Table 4
Adsorption isotherms constants for the adsorption of Bezactiv Orange on chitosan/MMT membranes.

Sample	Langmuir isotherm			Freundlich isotherm		
	R^2	Q_{max} (mg/g)	K_l (L/mg)	R^2	$1/n$	K_f (mg/g)
Chitosan/MMT 10%	0.92	106.8	0.210	0.99	0.321	34.1
Chitosan/MMT 20%	0.93	128.7	0.159	0.99	0.293	37.8
Chitosan/MMT 30%	0.91	277.7	0.0542	0.99	0.654	21.1
Chitosan/MMT 40%	0.92	322.6	0.0749	0.99	0.639	30.8
Chitosan/MMT 50%	0.88	740.7	0.0247	0.97	0.854	20.4

Table 5
The comparison of adsorption capacities of the system reported in this paper with similar adsorbents from the literature.

Reference	Adsorbent	Dye		Concentration of dye (mg/L)	Q_{max} (mg/g)	
This work	Chitosan/MMT membrane	Bezactiv Orange		80	279	
[18]	Na-bentonite Kaolin Zeolite	Congo red		150	7.29 5.58 3.03	
[49]	Chitosan-crosslinked beads	Reactive Orange 16 (Bezactiv Orange)		100	30	
[50]	Organofunctionalized kenyaite	Bezactiv Orange		80	33.9	
[24]	Chitosan Na-MMT Chitosan–MMT beads	Basic Blue 9 Basic Blue 9 Basic Blue 9	Basic Yellow Basic Yellow Basic Yellow	500	44.2 42.1 48.9	25.1 24.7 45.9
[51]	Chitosan–bentonite beads	Tartrazine		60	245	
[52]	Quaternary chitosan salt cross-linked (powder)	Bezactiv Orange		500 1000	500 1090	
[53]	Activated carbonaceous materials Non-activated carbonaceous materials	Bezactiv Orange		600	239 229	

Langmuir equation. The $1/n$ parameter of the Freundlich increased by increasing of content of MMT in membrane, and indicated that the membrane with higher content of MMT is more homogenous. Similar results are observed by SEM.

Adsorption capacities of chitosan, clays and modified chitosan adsorbents, reported in the literature, are reported in Table 5. The chitosan/MMT membranes exhibit a higher adsorption capacity at the significantly lower concentration comparing to the pure clays, which confirms the need to improve them with chitosan. Also, when compared to crosslinked forms of chitosan, and different adsorbent shapes (e.g. beads) it is visible that the uncrosslinked membrane form, used in this paper shows the highest adsorption potential.

4. Conclusion

The aim of this study was to characterize the polymer complexes based on chitosan and montmorillonite, and investigate their adsorption capability for removal of textile dyes. The adsorption kinetics of BO onto these membranes were investigated as a function of time, concentration, pH and temperature. Chitosan in combination with clays produced a very good adsorbent, decreasing chitosan drawbacks. These membranes had significantly higher adsorption capacity at the low acidic conditions (pH above 6), so it should not need wastewater pretreatment, which is the main advantage of these membranes in comparison to similar systems. Despite the relatively long adsorption time, these membranes are useful because of a very high adsorption capacity, and can be used for large scale applications where the dye output in wastewaters is a result of non-continuous processes. Due to the wide availability of both chitosan and MMT, these membranes are not expensive, and can be prepared onsite, wherever there is a need for that.

The dye adsorption capacity depended on the mass amount of MMT, with increasing capacity as the ratio of MMT increased. The increase of dye concentration in solution increases adsorption capacity. The results of adsorption kinetics and isotherms showed that the adsorption process can be fitted by the pseudo-second order equation and Freundlich equation, respectively. The intra-particle diffusion model confirmed that intra-particle diffusion is involved in the adsorption process, but is not the only rate controlling step. FTIR results and SEM micrographs also confirmed adsorption of Bezactiv Orange on chitosan/MMT membranes. The adsorption capacity decreased with temperature increase of the solution for the samples with 30, 40 and 50% amount of MMT in membrane. The investigated new material exhibits high adsorption capacity at low concentration of dye and very low mass of adsorbent, and is more efficient than the other adsorbents used for removal of Bezactiv Orange.

Acknowledgment

The authors acknowledge funding from the Ministry of Science, Technology and Development of the Republic Serbia, Science Project No. 43009.

References

[1] M.S. Chiou, H.Y. Li, Equilibrium and kinetic modeling of adsorption of reactive dye on cross-linked chitosan beads, J. Hazard. Mater. B93 (2002) 233–248.
[2] E.K. Raymound, F. Dunald, Encyclopedia of Chemical Technology, John Wiley, New York, USA, 1984.
[3] P. Nigam, G. Armour, I.M. Banat, D. Singh, R. Marchant, Physical removal of textile dyes and solid state fermentation of dye adsorbed agricultural residues, Bioresour. Technol. 72 (2000) 219–226.
[4] B. Stephen, C.P. Chiu, G.H. Ho, J. Yang, B.H. Chen, Removal of cationic dyes from aqueous solution using an anionic poly-γ-glutamic acid-based adsorbent, J. Hazard. Mater. 137 (1) (2006) 226–234.
[5] X.Y. Yang, B. Al-Duri, Application of branched pore diffusion model in the adsorption of reactive dyes on activated carbon, Chem. Eng. J. 83 (2001) 15–23.
[6] G. McKay, The adsorption of dyestuffs from aqueous solution using activated carbon: analytical solution for batch adsorption based on external mass transfer and pore diffusion, Chem. Eng. J. 27 (1983) 187–196.
[7] F. Rozada, L.F. Calvo, A.I. Garcia, J. Martin-Villacorta, M. Otero, Dye adsorption by sewage sludge-based activated carbons in batch and fixed-bed systems, Bioresour. Technol. 87 (2003) 221–230.

[8] B.S. Inbaraj, C.P. Chiu, G.H. Ho, J. Yang, B.H. Chen, Effects of temperature and pH on adsorption of basic brown 1 by the bacterial biopolymer poly(γ-glutamic acid), Bioresour. Technol. 99 (2008) 1026–1035.
[9] B.S. Inbaraj, J.T. Chien, G.H. Hob, J. Yang, B.H. Chen, Equilibrium and kinetic studies on sorption of basic dyes by a natural biopolymer poly(γ-glutamic acid), Biochem. Eng. J. 31 (2006) 204–215.
[10] S.M.O. Brito, H.M.C. Andrade, L.F. Soares, R.P. Azevedo, Brazil nut shells as a new biosorbent to remove methylene blue and inigo carmine from aqueous solution, J. Hazard. Mater. 174 (1–3) (2010) 84–92.
[11] Zh. Zhang, S. Xia, X. Wang, A. Yang, B. Xu, L. Chen, Zh. Zhu, J. Zhao, N. Jaffrezic-Renault, D. Leonard, A novel biosorbent for dye removal: extracellular polymeric substance (EPS) of Proteus mirabilis TJ-1, J. Hazard. Mater. 163 (2009) 279–284.
[12] F. Wu, R. Tseng, R. Juang, Kinetic modeling of liquid-phase adsorption of reactive dyes and metal ions on chitosan, Water Res. 35 (2001) 613–618.
[13] I. Uzun, Kinetics of the adsorption of reactive dyes by chitosan, Dyes Pigments 70 (2006) 76–83.
[14] R.G. Harris, J.D. Wells, B.B. Johnson, Selective adsorption of dyes and other organic molecules to kaolinite and oxide surfaces, Colloids Surf. A: Physicochem. Eng. Aspects 180 (2001) 131–140.
[15] V. Meshko, L. Markovska, M. Mincheva, A.E. Rodrigues, Adsorption of basic dyes on granular activated carbon and natural zeolite, Water Res. 35 (2001) 3357–3366.
[16] A. Gurses, S. Karaca, C. Dogar, R. Bayrak, M. Acikyildiz, M. Yalcin, Determination of adsorptive properties of clay/water system: methylene blue sorption, J. Colloid Interface Sci. 269 (2004) 310–314.
[17] M. Dogan, Y. Ozdemir, M. Alkan, Adsorption kinetics and mechanism of cationic methyl violet and methylene blue dyes onto sepiolite, Dyes Pigments 75 (2007) 701–713.
[18] A.S. Ozcan, B. Erdem, A. Ozcan, Adsorption of Acid Blue 193 from aqueous solutions onto BTMA-bentonite, Colloids Surf. A: Physicochem. Eng. Aspects 266 (2005) 73–81.
[19] V. Vimonsesa, Sh. Lei, B. Jina, Ch.W.K. Chowd, Ch. Saintb, Kinetic study and equilibrium isotherm analysis of Congo Red adsorption by clay materials, Chem. Eng. J. 148 (2009) 354–364.
[20] O. Ozdemir, B. Armagan, M. Turan, M.S. Celik, Comparison of the adsorption characteristics of azo-reactive dyes on mezoporous minerals, Dyes Pigments 62 (2004) 49–60.
[21] M. Darder, M. Colilla, E. Ruiz-Hitzky, Chitosan–clay nanocomposites: application as electrochemical sensors, Appl. Clay Sci. 28 (2005) 199–208.
[22] J.-H. An, S. Dultz, Adsorption of tannic acid on chitosan–montmorillonite as a function of pH and surface charge properties, Appl. Clay Sci. 36 (2007) 256–264.
[23] Sh. Hua, H. Yang, W. Wang, A. Wang, Controlled release of ofloxacin from chitosan–montmorillonite hydrogel, Appl. Clay Sci. 50 (2010) 112–117.
[24] S. Kittinaovarat, P. Kansomwan, N. Jiratumnukul, Chitosan/modified montmorillonite beads and adsorption Reactive Red 120, Appl. Clay Sci. 48 (2010) 87–91.
[25] P. Monvisade, P. Siriphannon, Chitosan intercalated montmorillonite: preparation, characterization and cationic dye adsorption, Appl. Clay Sci. 42 (2009) 427–431.
[26] X. Jiang, L. Chen, W. Zhong, A new linear potentiometric titration method for the determination of deacetylation degree of chitosan, Carbohydr. Polym. 54 (2003) 457–463.
[27] S. Lagergren, About the theory of so-called adsorption of soluble substances, K. Sven. Vetenskapsakad. Handl. 24 (1898) 1–39.
[28] Y.S. Ho, G. McKay, The kinetics of sorption of basic dyes from aqueous solution by sphagnum moss peat, Can. J. Chem. Eng. 76 (1998) 822–827.
[29] W.J. Weber, J.C. Morris, Kinetics of adsorption on carbon from solution, J. Sanit. Eng. Div. Am. Soc. Civ. Eng. 89 (1963) 31–60.
[30] B. Tyagi, Ch. D. Chudasama, R.V. Jasra, Determination of structural modification in acid activated montmorillonite clay by FT-IR spectroscopy, Spectrochim. Acta Part A 64 (2006) 273–278.
[31] N.B. Milosavljevic, Lj.M. Kljajevic, I.G. Popovic, J.M. Filipovic, M.T. Kalagasidis Krusic, Chitosan, itaconic acid and poly(vinylalcohol) hybrid polymer networks of high degree of swelling and good mechanical strength, Polym. Int. 59 (2010) 686–694.
[32] T. Wang, M. Turhan, S. Gunasekaran, Selected properties of pH-sensitive, biodegradable chitosan–poly(vinylalcohol) hydrogel, Polym. Int. 53 (2004) 911–918.
[33] R.H. Marchessault, F. Ravenelle, X.X. Zhu, Polysaccharides for Drug Delivery and Pharmaceutical Applications, vol. 934, American Chemical Society, 2006, p. 368.
[34] M.L. Duarte, M.C. Ferreira, M.R. Marvao, J. Rocha, Int. J. Biol. Macromol. 31 (2002) 1–8.
[35] S.S. Ray, K. Okamoto, M. Okamoto, Macromolecules 36 (2003) 2355–2367.
[36] M. Darder, M. Colilla, E. Ruiz-Hitzky, Biopolymer–clay nanocomposites based on chitosan intercalated in montmorillonite, Chem. Mater. 15 (2003) 3774–3780.
[37] C. Paluszkiewicza, E. Stodolakb, M. Hasika, M. Blazewiczb, FT-IR study of montmorillonite–chitosan nanocomposite materials, Spectrochim. Acta Part A 79 (2010) 784–788.
[38] K.L. Shantha, P. Ravichandran, K. Panduranga Rao, Azo polymeric hydrogels for colon targeted drug delivery, Biomaterials 16 (17) (1995) 1313–1318.
[39] Y.S. Han, S.H. Lee, K.H. Choi, I. Park, Preparation and characterization of chitosan–clay nanocomposites with antimicrobial activity, J. Phys. Chem. Solids 71 (2010) 464–467.
[40] S.F. Wang, L. Chen, Y. Tong, Structure–property relationship in chitosan-based biopolymer/montmorillonite nanocomposites, J. Polym. Sci. A 44 (1) (2006) 686–696.
[41] S.F. Wang, L. Shen, Y.J. Tong, L. Chen, I.Y. Phang, P.Q. Lim, T.X. Liu, Biopolymer chitosan/montmorillonite nanocomposites: preparation and characterization, Polym. Degrad. Stab. 90 (2005) 121–131.
[42] Ch. Tang, N. Chen, Q. Zhang, K. Wang, Q. Fu, X. Zhang, Preparation and properties of chitosan nanocomposites with nanofillers of different dimensions, Polym. Degrad. Stab. 94 (2009) 124–131.
[43] L. Abramian, H. El-Rassy, Adsorption kinetics and thermodynamics of azo-dye Orange II onto highly porous titania aerogel, Chem. Eng. J. 150 (2009) 403–410.
[44] Z. Cheng, X. Liu, M. Han, W. Ma, Adsorption kinetic character of copper ions onto a modified chitosan transparent thin membrane from aqueous solution, J. Hazard. Mater. 182 (2010) 408–415.
[45] K. Ravikumar, B. Deebika, K. Balu, Decolourization of aqueous dye solutions by a novel adsorbent: application of statistical designs and surface plots for the optimization and regression analysis, J. Hazard. Mater. B1222 (2005) 75–83.
[46] V. Singha, A.K. Sharmaa, R. Sanghib, Poly(acrylamide) functionalized chitosan: an efficient adsorbent for azo dyes from aqueous solutions, J. Hazard. Mater. 166 (2009) 327–335.
[47] V. Singha, A.K. Sharmaa, D.N. Tripathi, R. Sanghib, Poly(methylmethacrylate) grafted chitosan: an efficient adsorbent for anionic azo dyes, J. Hazard. Mater. 161 (2009) 955–966.
[48] M.M. Dávila-Jimenez, M.P. Elizalde-Gonzalez, A.A. Peláez-Cid, Adsorption interaction between natural adsorbents and textile dyes in aqueous solution, Colloid Int. Sci. A 254 (1–3) (2005) 107–114.
[49] Y. Kimura, M.C.M. Laranjeira, V.T. Fávere, L. Furlan, The interaction between reactive dye containing vinylsulfone group and chitosan microspheres, Int. J. Polym. Mater. 51 (2002) 759–768.
[50] B. Royer, N.F. Cardoso, E.C. Lima, V.S.O. Ruiz, Th.R. Macedo, C. Airoldi, Organofunctionalized kenyaite for dye removal from aqueous solution, Colloid Int. Sci. 336 (2009) 398–405.
[51] W.S. Wan Ngah, N. Farhana Md Ariff, M.A.K. Megat Hanafiah, Preparation, characterization, and environmental application of crosslinked chitosan-coated bentonite for tartrazine adsorption from aqueous solutions, Water Air Soil Pollut. 206 (2010) 225–236.
[52] S. Rosa, M.C.M. Laranjeira, H.G. Riela, V.T. Favere, Cross-linked quaternary chitosan as an adsorbent for the removal of the reactive dye from aqueous solutions, J. Hazard. Mater. 155 (2008) 253–260.
[53] T. Calvete, E.C. Lima, N.F. Cardoso, J.C.P. Vaghetti, S.L.P. Dias, F.A. Pavan, Application of carbon adsorbents prepared from Brazilian-pine fruit shell for the removal of reactive orange 16 from aqueous solution: kinetic, equilibrium, and thermodynamic studies, J. Environ. Manage. 91 (2010) 1695–1706.